



## NRC Publications Archive Archives des publications du CNRC

### **Hot corrosion of lanthanum zirconate and partially stabilized zirconia thermal barrier coatings**

Marple, Basil R.; Voyer, Joël; Thibodeau, Michel; Nagy, Douglas R.; Vassen, Robert

This publication could be one of several versions: author's original, accepted manuscript or the publisher's version. / La version de cette publication peut être l'une des suivantes : la version prépublication de l'auteur, la version acceptée du manuscrit ou la version de l'éditeur.

For the publisher's version, please access the DOI link below. / Pour consulter la version de l'éditeur, utilisez le lien DOI ci-dessous.

#### **Publisher's version / Version de l'éditeur:**

<https://doi.org/10.1115/1.1924534>

*Journal of Engineering for Gas Turbines and Power*, 128, 1, pp. 144-152, 2006-01-01

#### **NRC Publications Record / Notice d'Archives des publications de CNRC:**

<https://nrc-publications.canada.ca/eng/view/object/?id=eac6802c-5dc9-4f76-95e0-7280f0249422>

<https://publications-cnrc.canada.ca/fra/voir/objet/?id=eac6802c-5dc9-4f76-95e0-7280f0249422>

Access and use of this website and the material on it are subject to the Terms and Conditions set forth at

<https://nrc-publications.canada.ca/eng/copyright>

READ THESE TERMS AND CONDITIONS CAREFULLY BEFORE USING THIS WEBSITE.

L'accès à ce site Web et l'utilisation de son contenu sont assujettis aux conditions présentées dans le site

<https://publications-cnrc.canada.ca/fra/droits>

LISEZ CES CONDITIONS ATTENTIVEMENT AVANT D'UTILISER CE SITE WEB.

**Questions?** Contact the NRC Publications Archive team at

PublicationsArchive-ArchivesPublications@nrc-cnrc.gc.ca. If you wish to email the authors directly, please see the first page of the publication for their contact information.

**Vous avez des questions?** Nous pouvons vous aider. Pour communiquer directement avec un auteur, consultez la première page de la revue dans laquelle son article a été publié afin de trouver ses coordonnées. Si vous n'arrivez pas à les repérer, communiquez avec nous à PublicationsArchive-ArchivesPublications@nrc-cnrc.gc.ca.



**Basil R. Marple<sup>1</sup>**

e-mail: basil.marple@nrc.ca

**Joël Voyer<sup>2</sup>**

**Michel Thibodeau**

National Research Council Canada,  
Industrial Materials Institute,  
75 de Mortagne Boulevard,  
Boucherville, QC J4B 6Y4, Canada

**Douglas R. Nagy**

Liburd Engineering Limited,  
400 Highway 6 North,  
Dundas, ON L9H 7K4, Canada

**Robert Vassen**

Institute for Materials  
and Processes in Energy Systems,  
Forschungszentrum Jülich GmbH,  
D-52425 Jülich, Germany

# Hot Corrosion of Lanthanum Zirconate and Partially Stabilized Zirconia Thermal Barrier Coatings

*The hot corrosion resistance of lanthanum zirconate and 8 wt. % yttria-stabilized zirconia coatings produced by thermal spraying for use as thermal barriers on industrial gas turbines or in aerospace applications was evaluated. The two ceramic oxide coatings were exposed for various periods of time at temperatures up to 1000°C to vanadium- and sulfur-containing compounds, species often produced during the combustion of typical fuels used in these applications. Changes in the coatings were studied using a scanning electron microscope to observe the microstructure and x-ray diffraction techniques to analyze the phase composition. The results showed different behaviors for the two materials: the zirconia-based coating being rapidly degraded by the vanadium compounds and resistant to attack by the sulfur materials while the lanthanum zirconate was less damaged by exposure to vanadia but severely attacked in the presence of sulfur-containing species. [DOI: 10.1115/1.1924534]*

## 1 Introduction

Thermal barrier coatings (TBCs) are widely used in jet engines and land-based turbines as insulating layers to shield the underlying components from the high temperatures arising from combustion. The TBCs consist of a duplex structure comprised of a metallic bond coat and a ceramic top coat. The bond coat is applied directly to the roughened surface of the component and plays an important role in reducing oxidation of the high temperature metal alloy in the underlying part. The top coat is normally a porous layer of a ceramic oxide applied either by thermal spraying or by an electron beam physical vapor deposition (EB-PVD) process. It serves as a thermal insulator, reducing the temperature experienced by the surface of the underlying component during operation. The combination of internal air cooling using channels both within and at the back face of the component together with the insulating effect of the TBC can result in a temperature drop of approximately 150°C across the coating [1].

Because of the protection offered by the TBC, it is possible to extend the life of the underlying component and increase the cycle time between stoppages for overhaul and repair. This cycle time has been reported to be approximately 8000 h for commercial aircraft and 24,000 h for turbines used for power generation [2]. In these applications, TBCs are not currently required to serve as the “last line of defense” and most components can function for at least a short time without them. However, it is projected that new, higher-performance engines will be developed having higher operating temperatures and larger temperature drops across the TBC [1]. It is expected that at some point TBCs will become “prime reliant” parts of the system. In other words, failure of the coating would lead to failure, in some cases in a catastrophic fashion, of the underlying component.

The requirement for increased insulation to protect components

from hotter combustion gases will necessitate a change in the TBC system to achieve a higher temperature drop across the coating. Thicker ceramic coatings are one possible approach to improving the insulating value of the TBC [3,4]. However, producing thicker coatings presents challenges, particularly when deposited using plasma spraying, because of the build up of stresses that can cause the coating to spall. There are also concerns associated with the increased weight of thicker coatings and the possibility of creep at higher temperatures when the coatings are being employed on rotating components. And even if thicker coatings can be produced and employed on rotating components, there is a question concerning the ability of the most widely used top coat composition, 8 wt. %  $Y_2O_3$ - $ZrO_2$ , to resist sintering at the higher temperatures to which it will be exposed. Sintering and densification can degrade the coating [5] and raise the thermal conductivity, making it a less effective thermal barrier.

There is a need, therefore, for the development of new design strategies or new materials for TBCs in order to address the challenges of more demanding operating environments. One composition that has been shown to possess some very interesting properties for this application is lanthanum zirconate,  $La_2Zr_2O_7$  [6,7]. The results of early work have shown that this material has a stable phase structure and, when engineered correctly, can outperform a standard yttria-stabilized zirconia TBC in high-temperature thermal cycling tests [8].

The present study focuses on another aspect of the performance of these materials—resistance to hot corrosion. This is one of several degradation processes identified as contributing to the deterioration of TBCs [9]. Much of the body of work performed in the area of hot corrosion of TBCs was reviewed and summarized in a relatively recent paper by Jones [10]. Under normal operating conditions, hot corrosion of TBCs used in power generation and jet engine components arises due to reactions involving impurities, particularly vanadium, sulfur and sodium, present in the fuel. The present study compares the hot corrosion performance of  $ZrO_2$ -8 wt. %  $Y_2O_3$  and  $La_2Zr_2O_7$  in the presence of vanadium and sulfur compounds.

<sup>1</sup>To whom correspondence should be addressed.

<sup>2</sup>Currently at ARC Leichtmetallkompetenzzentrum GmbH, Ranshofen, Austria.

Contributed by the IGTI Manufacturing Materials and Metallurgy Committee of ASME for publication in the JOURNAL OF ENGINEERING FOR GAS TURBINES AND POWER. Manuscript received by the MM&M Committee February 8, 2004; final revision received July 30, 2004. IGTI Review Chair: W. Miglietti.

**Table 1 Spray parameters used to deposit the various TBC materials**

| Spray conditions         | Coating            |                  |  |   |
|--------------------------|--------------------|------------------|--|---|
|                          | Bond coat for 8YSZ | 8YSZ top coat    | Bond coat for La <sub>2</sub> Zr <sub>2</sub> O <sub>7</sub> | La <sub>2</sub> Zr <sub>2</sub> O <sub>7</sub> top coat |
| Process                  | APS <sup>a</sup>   | APS <sup>a</sup> | VPS <sup>b</sup>   | APS <sup>c</sup>  |
| Voltage (V)              | 37                 | 43               | 76   | 69  |
| Current (A)              | 700                | 400              | 650  | 300   |
| Primary Gas              | Ar                 | Ar               | Ar   | Ar  |
| Flow (lpm)               | 50.0               | 38.7             | 40   | 20  |
| Secondary Gas            | He                 | H <sub>2</sub>   | H <sub>2</sub>   | He  |
| Flow (lpm)               | 23.6               | 2.0              | 15   | 13  |
| Carrier Gas              | Ar                 | Ar               | Ar   | Ar  |
| Flow (lpm)               | 6.5                | 8.6              | 1.7  | 2.5   |
| Powder Feed Rate (g/min) | 17.0               | 22.6             | 38.4   | 27.0  |
| Spray Distance (cm)      | 6.4                | 6.4              | 27.5   | 9.0   |

<sup>a</sup>SG-100 plasma spray gun, Praxair Surface Technologies, Concord, NH.<sup>b</sup>F4 Plasma Spray Gun, Sulzer Metco, Wohlen, Switzerland.<sup>c</sup>Triplex I Plasma Spray Gun, Sulzer Metco, Wohlen, Switzerland.

## 2 Experimental Procedure

**2.1 Thermal Spray Processing.** Coatings were produced by plasma spraying onto 19 mm diameter metal substrates containing Ni as the major element and Cr, Mo, Nb, and Fe as the principal minor constituents (IN-625, Rolled Alloys, Mississauga, Canada). Before depositing the coatings, the surface of the substrate was roughened by grit blasting with alumina particles. To produce the bond coat, a Ni–Cr–Al–Y alloy (Ni-164-2, Praxair Surface Technologies, Indianapolis, IN) was deposited to a thickness of ap-

proximately 150–220  $\mu\text{m}$  using two different processes. For the TBC system designed to have a zirconia-based top coat, the bond coat was produced by atmospheric plasma spraying (APS) (SG-100 Plasma Spray Gun, Praxair Surface Technologies, Concord, NH). The bond coat for the TBC system involving La<sub>2</sub>Zr<sub>2</sub>O<sub>7</sub> as the ceramic top coat was deposited using vacuum plasma spraying (VPS). This was accomplished using a plasma spray gun (Model F4, Sulzer Metco, Wohlen, Switzerland) mounted in a VPS unit manufactured by the same company.

The ceramic top coats were deposited onto the bond coat to a thickness of approximately 250  $\mu\text{m}$  using two different APS systems. The zirconia-based TBC top coat was produced using a yttria-stabilized zirconia powder containing 8 wt. % yttrium oxide and having a reported size distribution in the range 10–106  $\mu\text{m}$  (204NS, Sulzer Metco, Westbury, NY). This was accomplished using the same APS gun as used for depositing the bond coat for this TBC system. In the remaining sections of this paper this yttria-stabilized zirconia top coat will be referred to as 8YSZ, a designation now widely used in the TBC literature. The lanthanum zirconate top coat was deposited using a second APS system (Triplex I Plasma Spray Gun, Sulzer Metco, Wohlen, Switzerland) and an experimental powder being developed and evaluated for use as a TBC material [6–8]. The spray conditions employed for depositing the various coatings are shown in Table 1.

**2.2 Hot Corrosion Testing.** Testing was performed to compare the changes in these coatings when exposed to compounds containing either vanadium or sulfur at elevated temperatures. A detailed description of the approach used to perform these types of tests is presented elsewhere [11]. To briefly summarize, the corrosion tests in the presence of vanadium compounds were performed by placing approximately 3.5 mg of high-purity V<sub>2</sub>O<sub>5</sub> powder on a 0.25 cm<sup>2</sup> area of the surface of the TBC and heating

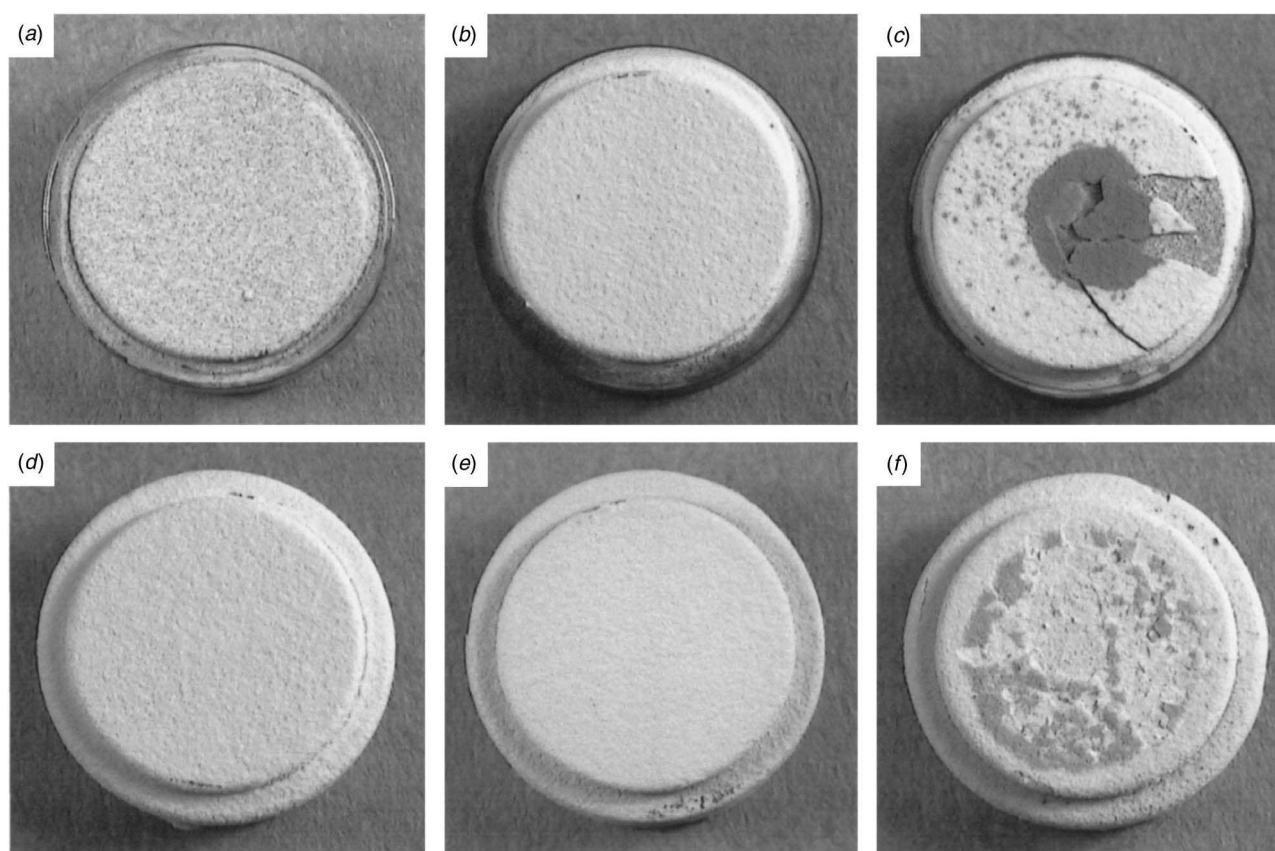


**Fig. 1 Overall appearance of the 8YSZ (a–c) and La<sub>2</sub>Zr<sub>2</sub>O<sub>7</sub> (d–f) TBCs at various stages: in the as-deposited state (a) and (d), after a 3-h dwell at 1000°C (b) and (e), and following a 3-h corrosion test at 1000°C in contact with V<sub>2</sub>O<sub>5</sub> (c) and (f)**



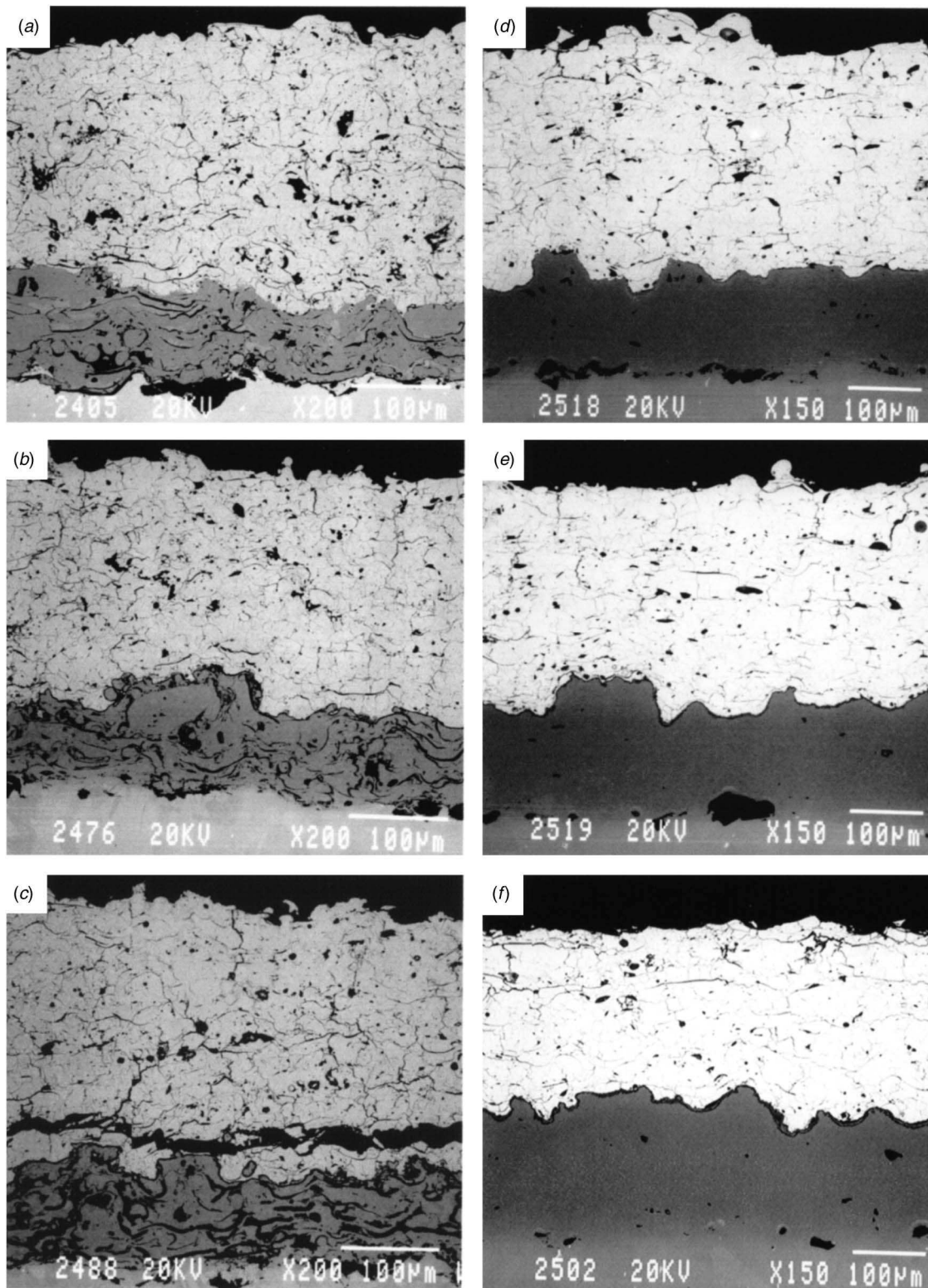


**Fig. 2** Structure of 8YSZ (*a–c*) and  $\text{La}_2\text{ZrO}_7$  (*d–f*) coatings in the as-sprayed state (*a* and *d*), after 3 h at  $1000^\circ\text{C}$  (*b* and *e*), and following contact with  $\text{V}_2\text{O}_5$  at  $1000^\circ\text{C}$  for 3 h (*c* and *f*)

( $600^\circ\text{C}/\text{h}$ ) the sample in a furnace to  $1000^\circ\text{C}$  in ambient air. Following a 3-h dwell under these conditions, the samples were left to cool in the furnace. Samples that had not been treated with  $\text{V}_2\text{O}_5$  powder were subjected to an identical heat treatment.

Exposure of the TBCs to sulfur compounds was performed by applying sulfate salts and then heating the samples in a furnace to  $900^\circ\text{C}$  under a flow of  $\text{SO}_2$ -containing dried air. This was accom-

plished by first cleaning the TBC and then performing a salting procedure involving heating the samples in a furnace to  $300^\circ\text{C}$  and then spraying the hot coating with a salt solution (containing sulfate salts in a mole ratio of  $3\text{Na}_2\text{SO}_4:2\text{MgSO}_4$ ) to achieve a salt coverage of  $4\text{ mg}/\text{cm}^2$ . These samples (two from each composition) were then heated in a furnace at  $900^\circ\text{C}$  under a gas flow consisting of  $2000\text{ ml}/\text{min}$  of dried air and  $5\text{ ml}/\text{min}$  of  $\text{SO}_2$ . An

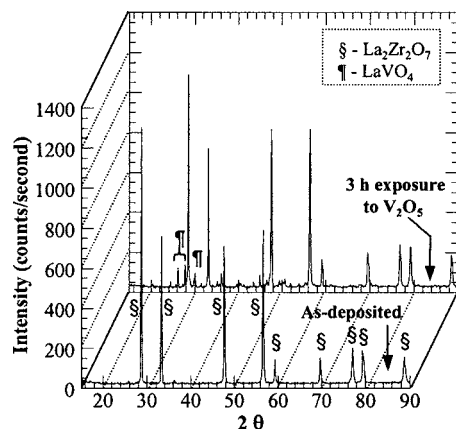


**Fig. 3** X-ray diffraction spectra for the  $\text{La}_2\text{Zr}_2\text{O}_7$  coating in the as-sprayed state and following a 3-h treatment at  $1000^\circ\text{C}$  in contact with  $\text{V}_2\text{O}_5$

exposure interval of 20 h was employed, following which the samples were removed, inspected and resalted. The samples were then reinserted into the furnace for another 20-h interval. When significant degradation of a coating was observed during the inspection step, one of the samples of that composition was removed from the corrosion test for further analysis. A total exposure at  $900^\circ\text{C}$  of up to 360 h was employed for some samples.

Another test was performed to determine the combined effect of sulfur and vanadium compounds on these TBC materials when exposed simultaneously to these two substances at elevated temperatures. For this test, a dry mixture comprised of 85 wt. %  $\text{Na}_2\text{SO}_4$  and 15 wt. %  $\text{V}_2\text{O}_5$  was placed on the TBC to a coverage of  $4 \text{ mg}/\text{cm}^2$ . These samples were heated in a furnace at  $900^\circ\text{C}$  under the same gas flow described above using an exposure interval of 20 h. After each interval, the samples were inspected, resalted and then reinserted into the furnace. However, if there was significant degradation of a coating, the sample was not subjected to any further exposure to the corrosive conditions. Maximum exposure time for these samples was 60 h.

**2.3 Characterization.** Coatings were studied using a scanning electron microscope (SEM) and x-ray diffraction (XRD) techniques. To characterize the changes in microstructure during the hot corrosion tests, polished cross sections of resin vacuum-impregnated samples of the as-sprayed, heat-treated and corroded samples were observed under an SEM (JSM-6100, JEOL, Tokyo, Japan). The SEM was equipped with an energy dispersive x-ray spectrometer (EDS) (Analyzer eXL, Link Systems, High Wycombe, U.K.), which was used to obtain information on the distribution of the various elements within the samples. The phases present in the various samples were identified by XRD (Model D8, Bruker AXS, Karlsruhe, Germany) using  $\text{Cu } K\alpha$  radiation, a step size of  $0.1^\circ$ , a step time of 0.5 s and a  $2\theta$  scan window from  $15^\circ$  to  $90^\circ$ .

### 3 Results

**3.1 Corrosion by Vanadium Compounds.** The overall appearance of the two groups of samples used to determine the effect of exposure to vanadium compounds is shown in Fig. 1. It is apparent that, as observed in earlier work [11], the presence of  $\text{V}_2\text{O}_5$  has a negative effect on the 8YSZ coating, which results in a serious degradation. Whereas the as-sprayed (Fig. 1(a)) and heat-treated (Fig. 1(b)) 8YSZ coatings appeared to be well bonded to the substrate, delamination and spalling of the ceramic top coat is apparent in Fig. 1(c). The dark stain seen on this coating was maroon in color and was caused by the reaction and spreading of

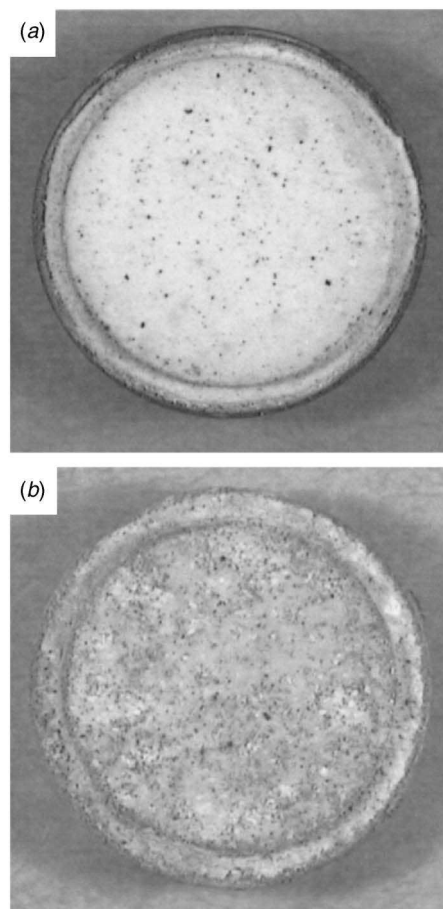


**Fig. 4** Photographs of the coated test specimens following 360 h of exposure to sulfur-containing salts at  $900^\circ\text{C}$ : (a)  $\text{ZrO}_2$ -8 wt. %  $\text{Y}_2\text{O}_3$  and (b)  $\text{La}_2\text{Zr}_2\text{O}_7$

the  $\text{V}_2\text{O}_5$ .

In the case of the  $\text{La}_2\text{Zr}_2\text{O}_7$  top coat, a simple heat treatment at  $1000^\circ\text{C}$  did not appear to cause a significant change in the coating or lead to debonding (Figs. 1(d) and 1(e)). When this treatment was performed in the presence of  $\text{V}_2\text{O}_5$ , a green-colored substance (gray deposits seen in Fig. 1(f)) was observed on the surface of the coating following the test. However, any reactions that may have occurred during the corrosion test did not appear to have affected the bonding of the TBC to the substrate.

Micrographs of the cross sections of the six samples shown in Fig. 1 are presented in Fig. 2. The micrographs show that both top coat compositions have a stable microstructure, exhibiting little change when subjected to a heat treatment at  $1000^\circ\text{C}$  (compare Figs. 2(a), 2(b), 2(d), and 2(e)). This was also observed at higher magnifications (not shown). The micrographs shown in Figs. 2(c) and 2(f) confirm the observation from Fig. 1 concerning the effect of exposure of the TBCs to  $\text{V}_2\text{O}_5$  at  $1000^\circ\text{C}$  on bonding; delamination of the 8YSZ occurs in the ceramic layer just above the bond coat (Fig. 2(c)) and the  $\text{La}_2\text{Zr}_2\text{O}_7$  remains well bonded to the substrate (Fig. 2(f)).

Results of element mapping for the samples exposed to  $\text{V}_2\text{O}_5$  indicated that, in the case of 8YSZ, significant infiltration of the vanadium compound into the top coat had occurred. In the case of  $\text{La}_2\text{Zr}_2\text{O}_7$ , overlap of the  $K_\alpha$  peak for vanadium and the  $L_{\beta 1}$  peak for lanthanum made it difficult to determine the distribution of vanadium using this technique.

Earlier XRD work showed that for 8YSZ, the phase present in the as-sprayed coating and in a coating heated at  $1000^\circ\text{C}$  was tetragonal zirconia. However, heating in contact with  $\text{V}_2\text{O}_5$ , pro-



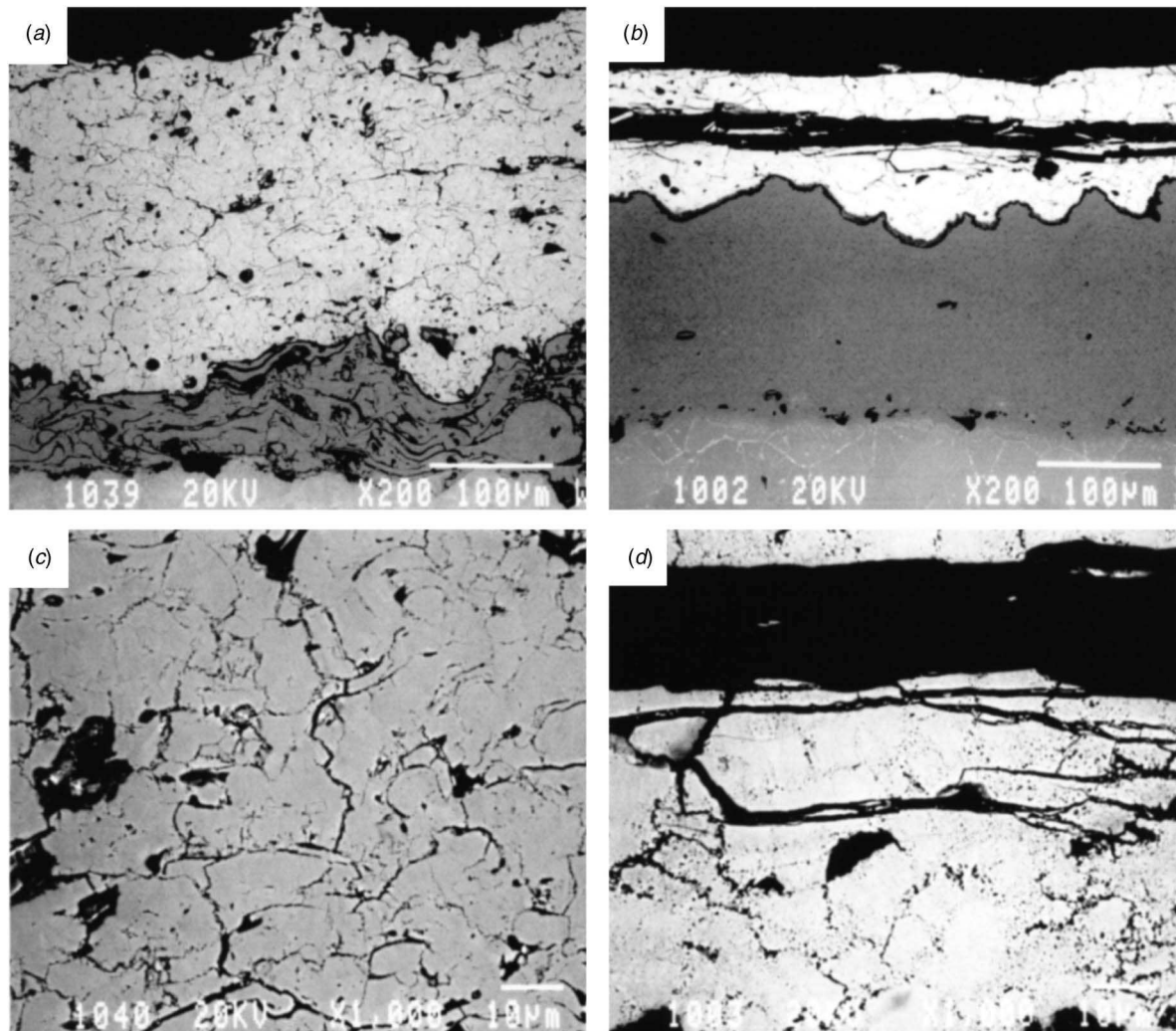


**Fig. 5** Micrographs of the coated test specimens following 360 h of exposure to sulfur-containing salts at 900°C: (a) and (c)  $\text{ZrO}_2$ -8 wt. %  $\text{Y}_2\text{O}_3$  and (b) and (d)  $\text{La}_2\text{Zr}_2\text{O}_7$

duced peaks attributed to monoclinic zirconia and to  $\text{YVO}_4$ . These results, presented elsewhere [11], were reconfirmed in the present work.

For the coating produced using a lanthanum zirconate powder, XRD analysis indicated that the as-sprayed coating exhibited peaks of a defect fluorite structure while the feedstock showed peaks characteristic of a stoichiometric  $\text{La}_2\text{Zr}_2\text{O}_7$  pyrochlore. As found earlier, the as-sprayed coatings transform into the pyrochlore structure after annealing at 1400°C and below [12]. Exposure of the coating to  $\text{V}_2\text{O}_5$  at 1000°C resulted in the appearance of peaks attributed to  $\text{LaVO}_4$  together with the additional pyrochlore peaks (Fig. 3). However, this new  $\text{LaVO}_4$  phase was present as a minor component and its appearance did not have the disruptive effect on the integrity of the coating as that observed with the YSZ material.

**3.2 Corrosion by Sulfur Compounds.** The overall appearance of the YSZ and the  $\text{La}_2\text{Zr}_2\text{O}_7$  coatings following the hot corrosion test in the presence of sulfur compounds can be seen in Fig. 4. While the  $\text{La}_2\text{Zr}_2\text{O}_7$  material experienced severe attack, the YSZ underwent little change following this 360-h treatment at 900°C. More detailed information on the level of attack can be obtained by observing the micrographs presented in Fig. 5 showing a cross-sectional view of the coatings at two levels of magnification. The YSZ coating has remained intact, with little change in the microstructure (compare to Fig. 2(a)). No major changes

were observed in the XRD spectra from that of the as-sprayed coating except for the appearance of very minor peaks at  $2\theta$  values in the range 28 deg to 29 deg and 31 deg to 32 deg. These peaks were attributed to the presence of monoclinic  $\text{ZrO}_2$  produced during the high-temperature corrosion test.

The  $\text{La}_2\text{Zr}_2\text{O}_7$  coating shown in Fig. 5(b) experienced severe cracking and delamination, reducing its thickness by more than half during the test (compare to Fig. 2(d)). As shown in Fig. 6 for a sample subjected to a 4.5-h test, degradation of this coating occurred rapidly under the conditions used in this study. The X-ray spectrum for the coating shown in Fig. 5(b) is presented in Fig. 7. By comparing this result to the spectrum of the as-sprayed coating shown in Fig. 3, it can be observed that the major change following heat treatment is the presence of peaks attributed to MgO. This material is the residue from decomposition of the sulfate salts used in the corrosion test. The absence of other compounds or phases suggests that either the coating was degraded by reactions producing volatile phases, if the attack was of a chemical nature, or, other factors contributed to deterioration of the coating.

**3.3 Corrosion in the Presence of both Vanadium and Sulfur Compounds.** The condition of the two coatings following exposure to a combination of sulfur and vanadium compounds can be seen in Fig. 8. Due to the significant degradation of the  $\text{La}_2\text{Zr}_2\text{O}_7$  material following the first 20 h of exposure, the test

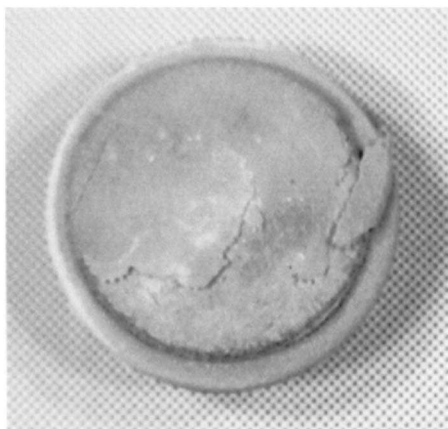


**Fig. 6** Photograph of a  $\text{La}_2\text{Zr}_2\text{O}_7$  coating following only 4.5 h of exposure to sulfur-containing compounds at  $900^\circ\text{C}$

was terminated for this sample at that point. The YSZ sample was subjected to two additional 20-h intervals, for a total exposure time of 60 h. Micrographs of the polished cross-sections of these samples are shown in Fig. 9. It is clear that both coatings were affected by this treatment. Although the bulk of the YSZ sample has remained on the substrate, delamination has begun, as evidenced by the relatively large crack located near the surface of the coating. The  $\text{La}_2\text{Zr}_2\text{O}_7$  material was much more severely degraded, with more than half of the coating having been removed (compare Figs. 1(b) and 2(d)). The EDS maps shown in Fig. 10 indicate that vanadium is present within both coatings. Similar maps for sulfur did not reveal the presence of this material within the coatings.

The x-ray spectra for these coatings together with those for the as-sprayed coatings are shown in Fig. 11. The spectra for YSZ (Fig. 11(a)) show that the zirconia has been almost completely transformed from the tetragonal to the monoclinic phase during the corrosion test. In the case of  $\text{La}_2\text{Zr}_2\text{O}_7$  (Fig. 11(b)), the material that remains following the corrosion test exhibits diffraction peaks little changed from the as-sprayed coating. Peaks are also found for a minor new phase identified as  $\text{LaVO}_4$ .

#### 4 Discussion

The results indicate that there are important differences between the hot corrosion resistance of 8YSZ and that of  $\text{La}_2\text{Zr}_2\text{O}_7$ . An 8YSZ coating is quite prone to attack by  $\text{V}_2\text{O}_5$  but relatively stable in the presence of sulfur-containing compounds. In contrast,  $\text{La}_2\text{Zr}_2\text{O}_7$  coatings are rapidly degraded when exposed to sulfur-containing compounds at  $900^\circ\text{C}$ ; however, contact with  $\text{V}_2\text{O}_5$

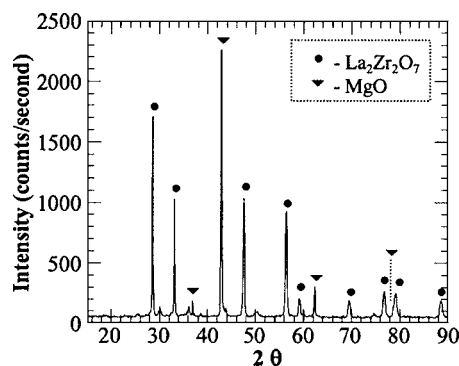


**Fig. 7** X-ray diffraction spectra for the  $\text{La}_2\text{Zr}_2\text{O}_7$  coating following 360 h of exposure to sulfur-containing salts at  $900^\circ\text{C}$  [sample shown in Fig. 5(b)].

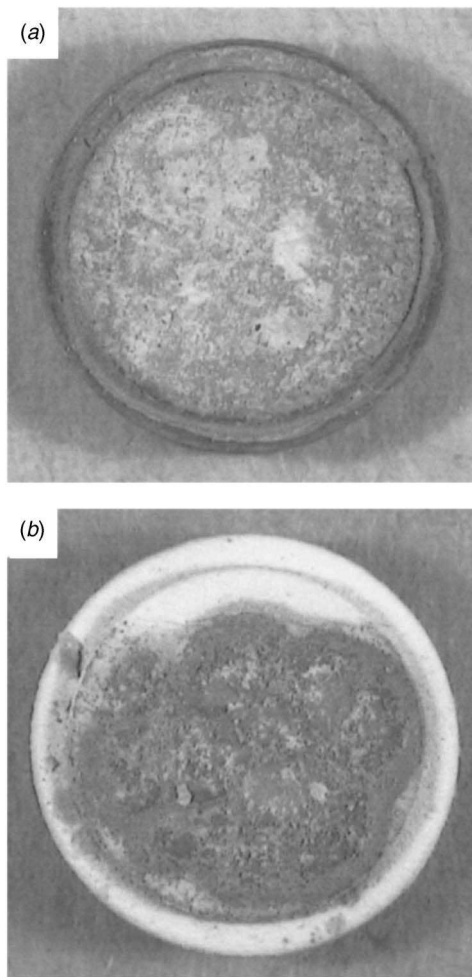


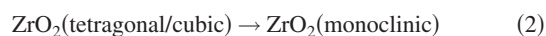
**Fig. 8** Appearance of the coatings following exposure to a combination of sulfur- and vanadium-containing compounds at  $900^\circ\text{C}$ : (a) YSZ after 60 h and (b)  $\text{La}_2\text{Zr}_2\text{O}_7$  after 20 h.

causes only very limited reaction at  $1000^\circ\text{C}$ . It is believed that the differences in performance of the two TBC systems can be explained solely on the basis of the difference in chemical composition of the tops coats and are not caused by the different thermal spray processes used to produce the bond coats and top coats.

The reactions that lead to the high-temperature degradation of yttria-stabilized zirconia coatings in the presence of vanadium compounds have been studied and explained by various other groups of researchers including Hamilton and Nagelberg [13] and Hertl [14] and discussed in earlier work by some of the present authors [11]. The yttria, added to zirconia to stabilize the tetragonal (and, in some cases, the cubic) zirconia structure, is attacked by vanadia via the following reaction:



As this reaction progresses, the amount of yttria remaining to serve as a stabilizing agent diminishes. Below a threshold yttria level, phase transformation of the zirconia will occur as represented by



This transformation would normally occur upon cooling and is accompanied by a volume expansion. These structural changes generate stresses that can cause cracking and fragmentation of the coating. In the present study it was shown that the  $\text{V}_2\text{O}_5$  (which melts at approximately  $690^\circ\text{C}$ ) infiltrated the porous ceramic layer to reach the bond coat. The subsequent reactions led to an



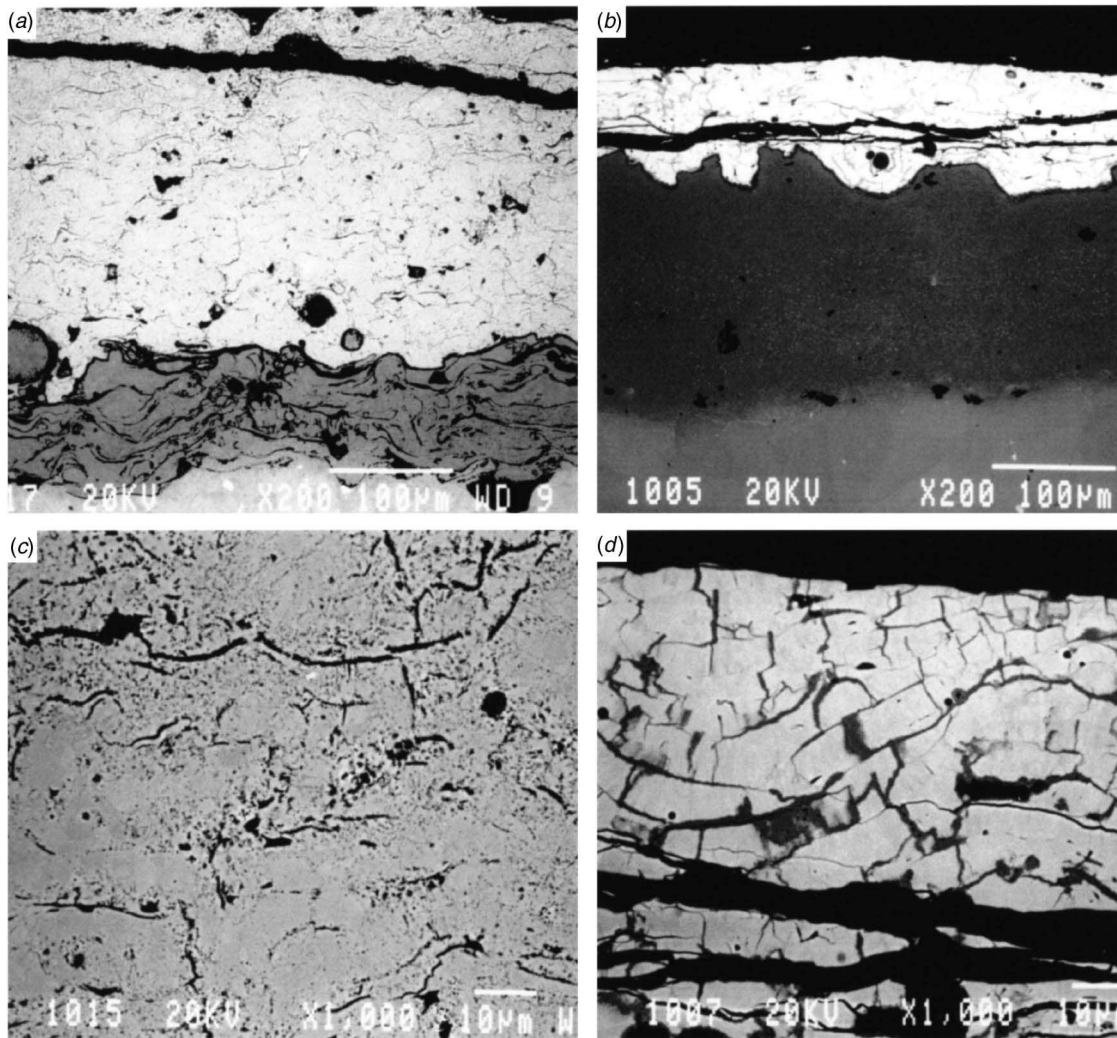


**Fig. 9 Micrographs of the cross section of coatings exposed to a combination of sulfur- and vanadium-containing compounds at 900°C: (a) and (c) YSZ after 60 h and (b) and (d)  $\text{La}_2\text{Zr}_2\text{O}_7$  after 20 h**

increased level of microcracking through the thickness of the coating (see Fig. 2(c)) and eventual spallation. The level of severity of attack was similar to that observed in earlier work [11]. It is worth noting that for YSZ samples in contact with vanadia, spallation typically occurred within 50  $\mu\text{m}$  of the interface between the top coat and the bond coat, indicating that the maximum (delamination) stresses generated by the changes occurring during the corrosion test were concentrated in this region. For the YSZ sample exposed to both sulfur- and vanadium-containing compounds, delamination was observed much nearer the surface of the top coat.

In the case of lanthanum zirconate only minor amounts of a new phase,  $\text{LaVO}_4$ , were detected following exposure to  $\text{V}_2\text{O}_5$ . A possible reaction that would have produced this phase can be written as



In contrast to the deleterious effect of vanadia on the 8YSZ coating, this reaction did not appear to have any major effect on the coating microstructure and did not lead to spallation of the coating. These preliminary results suggest that if resistance to exposure to vanadia, as might be the case when fuels containing a relatively high concentration of vanadium are employed, is a prime factor in selecting a TBC, then  $\text{La}_2\text{Zr}_2\text{O}_7$  would probably be a better candidate than 8YSZ.

The reactions with sulfur-containing compounds that led to the rapid degradation of the  $\text{La}_2\text{Zr}_2\text{O}_7$  coating could not be fully identified. In general the x-ray spectra (see Fig. 7) did not reveal the presence of new phases in the coating following the high-temperature tests in contact with sulfur salts. However, in one case, following a 40-h test, the oxysulfate  $\text{La}_2\text{O}_2\text{SO}_4$  was detected in the coating. A reaction leading to the formation of this species could be



It has been reported that at these temperatures (900°C) the oxysulfate rather than the sulfate,  $\text{La}_2(\text{SO}_4)_3$ , is the dominant species [15].

The occurrence of reaction (4) as part of the degradation sequence remains to be confirmed. However, these findings clearly show that, regardless of the mechanism of attack, in its current state this coating does not appear to be suitable for use in high-sulfur environments. Additional work is required to develop strategies such as the use of sealants or protective layers to improve the resistance of this material to hot corrosion by sulfur-containing compounds. Therefore, if one of the prime considerations in selecting a TBC material is high-temperature resistance to sulfur compounds (e.g., for use in applications involving the combustion



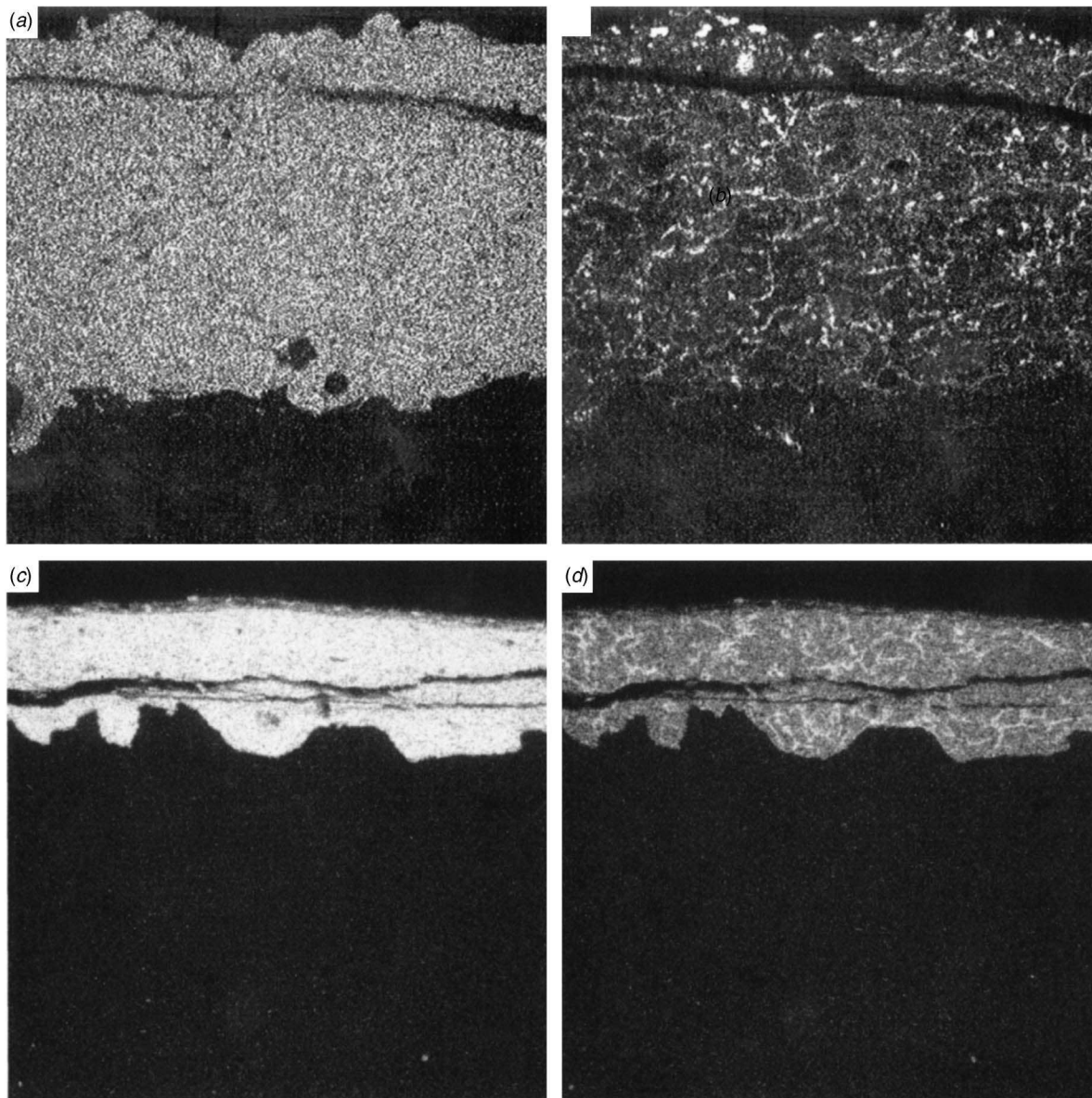


**Fig. 10** EDS dot maps showing the distribution of (a) zirconium and (b) vanadium in a region of the YSZ coating from the micrograph shown in Fig. 9(a) and maps for lanthanum (c) and vanadium (d) for a region of the  $\text{La}_2\text{Zr}_2\text{O}_7$  coating shown in Fig. 9(b). It is important to note that, due to the similarity of the energies for the  $V_{K\alpha}$  and  $\text{La}_{L\beta 1}$  peaks, the V map for the  $\text{La}_2\text{Zr}_2\text{O}_7$  coating has a component due to La.

of high-sulfur fuels), the results of this study indicate that 8YSZ would be a more suitable candidate than  $\text{La}_2\text{Zr}_2\text{O}_7$ .

It should be noted that in the search for new TBC materials to meet the needs of increasingly demanding operating conditions, hot corrosion is only one of the many factors that must be taken into account. Other aspects such as thermal conductivity, high-temperature phase stability, resistance to sintering/densification, compatibility with bond coat and substrate materials (in terms of both thermal expansion coefficient and chemistry), and mechanical properties are among those that must also be considered. Therefore, when designing TBC systems for specific service conditions, the results of this research on the hot corrosion resistance must be used in conjunction with those from studies in which other aspects of these materials were evaluated.

## 5 Summary and Conclusions

This study on the hot corrosion of  $\text{La}_2\text{Zr}_2\text{O}_7$  and yttria-stabilized zirconia thermal barrier coatings by vanadium- and

sulfur-containing compounds has shown a significant difference in the resistance of these materials to degradation by these two species. Lanthanum zirconate was relatively resistant to attack by vanadia. These coatings remained well bonded to the substrate following high-temperature exposure to this vanadium compound, contained only minor amounts of a new phase,  $\text{LaVO}_4$ , and exhibited a microstructure little changed from the as-sprayed state. For this same  $\text{La}_2\text{Zr}_2\text{O}_7$  material, contact with sulfate salts at  $900^\circ\text{C}$  resulted in very rapid disintegration of the coating, which occurred within 4 h under the conditions used in this work.

The performance of 8YSZ in the same tests was markedly different. Exposure to vanadia resulted in increased microcracking within the coating, reaction with the yttria stabilizer to produce  $\text{YVO}_4$ , an increase in the amount of monoclinic zirconia, and spallation of the coating. In contrast, this material exhibited excellent resistance to high-temperature attack by sulfate salts. Following 360 h of exposure to these species, the 8YSZ coating ap-

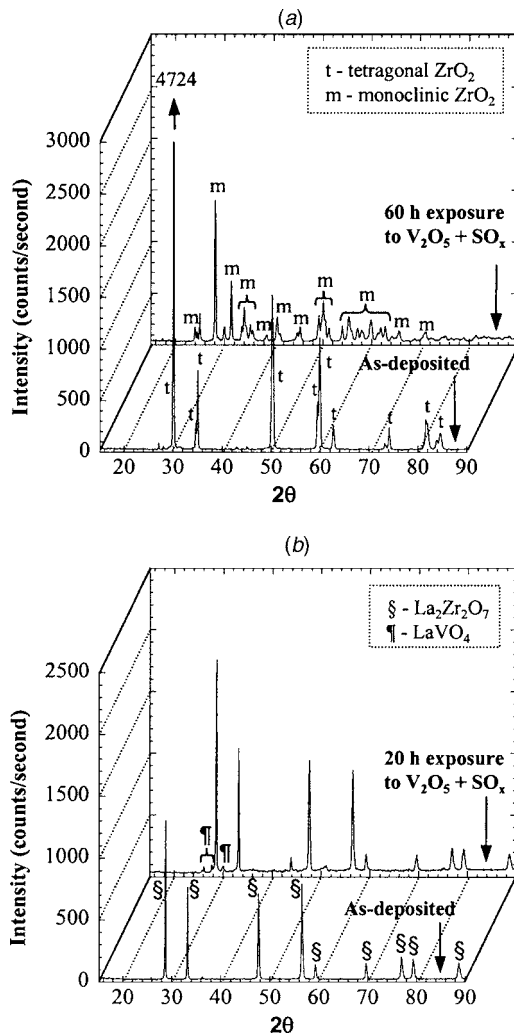


**Fig. 11 X-ray spectra for coatings in the as-sprayed state and following exposure to a combination of sulfur- and vanadium-containing compounds at 900°C: (a) YSZ and (b)  $\text{La}_2\text{Zr}_2\text{O}_7$**

peared to have maintained its structural integrity and remained well bonded to the substrate.

Not surprisingly, when the  $\text{La}_2\text{Zr}_2\text{O}_7$  and 8YSZ coatings were exposed to a mixture of vanadia and sulfate salts, both coatings

were degraded, the 8YSZ by vanadia and the  $\text{La}_2\text{Zr}_2\text{O}_7$  by the sulfate. These results underline the need for designing thermal barrier coatings taking into account the level of impurities in the fuel being used in the application and the operating conditions during service.

## Acknowledgment

The technical support of S. Bélanger, É. Poirier, and K. H. Rauwald during plasma spraying and sample preparation is gratefully acknowledged.

## References

- [1] Wigren, J., and Pejryd, L., 1998, "Thermal Barrier Coatings—Why, How, Where and Where To," *Thermal Spray—Meeting the Challenges of the 21st Century*, C. Coddet, ed., ASM International, Materials Park, OH, Vol. 2, pp. 1531–1542.
- [2] Nelson, W. A., and Orenstein, R. M., 1997, "TBC Experience in Land-Based Gas Turbines," *J. Therm. Spray Technol.*, **6**(2), pp. 176–180.
- [3] Beardsley, M. B., 1997, "Thick Thermal Barrier Coatings for Diesel Engines," *J. Therm. Spray Technol.*, **6**(2), pp. 181–186.
- [4] Steffens, H.-D., Babiak, Z., and Gramlich, M., 1999, "Some Aspects of Thick Thermal Barrier Coating Lifetime Prolongation," *J. Therm. Spray Technol.*, **8**(4), pp. 517–522.
- [5] Bose, S., and DeMasi-Marcin, J., 1997, "Thermal Barrier Coating Experience in Gas Turbine Engines at Pratt & Whitney," *J. Therm. Spray Technol.*, **6**(1), pp. 99–104.
- [6] Vaßen, R., Cao, X., Tietz, F., Kerkhoff, G., and Stöver, D., 1999, " $\text{La}_2\text{Zr}_2\text{O}_7$ —A New Candidate for Thermal Barrier Coatings," in *Proceedings of the United Thermal Spray Conference-UTSC'99*, E. Lugscheider and P. A. Kammer, eds., DVS-Verlag, Düsseldorf, Germany, pp. 830–834.
- [7] Vaßen, R., Cao, X., Tietz, F., Basu, D., and Stöver, D., 2000, "Zirconates as New Materials for Thermal Barrier Coatings," *J. Am. Ceram. Soc.*, **83**(8), pp. 2023–2028.
- [8] Vaßen, R., Cao, X., and Stöver, D., 2001, "Improvement of New Thermal Barrier Coating Systems Using a Layered or Graded Structure," *Ceram. Eng. Sci. Proc.*, **22**(4), pp. 435–442.
- [9] Lee, W. Y., Stinton, D. P., Berndt, C. C., Erdogan, F., Lee, Y.-D., and Mutasim, Z., 1996, "Concept of Functionally Graded Materials for Advanced Thermal Barrier Coating Applications," *J. Am. Ceram. Soc.*, **79**, pp. 3003–3012.
- [10] Jones, R. L., 1997, "Some Aspects of the Hot Corrosion of Thermal Barrier Coatings," *J. Therm. Spray Technol.*, **6**(1), pp. 77–84.
- [11] Marple, B. R., Voyer, J., Moreau, C., and Nagy, D. R., 2000, "Corrosion of Thermal Barrier Coatings by Vanadium and Sulfur Compounds," *Mater. High Temp.*, **17**(3), pp. 397–412.
- [12] Cao, X. Q., Vaßen, R., Jungen, W., Schwartz, S., Tietz, F., and Stöver, D., 2001, "Thermal Stability of Lanthanum Zirconate Plasma-Sprayed Coatings," *J. Am. Chem. Soc.*, **84**, pp. 2086–2090.
- [13] Hamilton, J. C., and Nagelberg, A. S., 1984, "In situ Raman Spectroscopic Study of Yttria-Stabilized Zirconia Attack by Molten Sodium Vanadate," *J. Am. Chem. Soc.*, **67**(10), pp. 686–690.
- [14] Hertl, W., 1988, "Vanadia Reactions with Yttria Stabilized Zirconia," *J. Appl. Phys.*, **63**(11), pp. 5514–5520.
- [15] Poston Jr., J. A., Siriwardane, R. V., Fisher, E. P., and Miltz, A. L., 2003, "Thermal Decomposition of the Rare Earth Sulfates of Cerium (III), Cerium (IV), Lanthanum (III), and Samarium (III)," *Appl. Surf. Sci.*, **214**, pp. 83–102.